

See discussions, stats, and author profiles for this publication at: <https://www.researchgate.net/publication/231274445>

# Predicting the Adsorption of Asphaltenes from Their Electrical Conductivity

ARTICLE *in* ENERGY & FUELS · NOVEMBER 2009

Impact Factor: 2.79 · DOI: 10.1021/ef900801n

---

CITATIONS

10

---

READS

39

2 AUTHORS, INCLUDING:



Lamia Goual

University of Wyoming

32 PUBLICATIONS 554 CITATIONS

SEE PROFILE

# Predicting the Adsorption of Asphaltenes from Their Electrical Conductivity

Lamia Goual\* and Adewunmi Abudu

Department of Chemical and Petroleum Engineering, University of Wyoming, Department 3295, 1000 East University Avenue, Laramie, Wyoming 82071

Received July 28, 2009. Revised Manuscript Received October 7, 2009

The adsorption of asphaltenes on solid surfaces can be the precursor of deposition problems in oilfields. The prediction of adsorption thickness using conventional techniques, such as quartz crystal microbalance (QCM), is usually costly and time-consuming. Alternatively, the adsorption can be related to asphaltene characteristics in the bulk phase that are easier to determine. This study investigates the relationship between the adsorption thickness of asphaltenes on hydrophilic surfaces, such as gold, and their electrical conductivity in toluene within a range of concentrations where adsorption is diffusion-controlled. The method is based on the measurement of direct-current (DC) conductivity of petroleum fluids in toluene using the impedance spectroscopy (IS) method. An inverse relationship is established between the thickness of adsorbed rigid monolayer films on gold and the conductivity of particles in the bulk fluid. However, the relation does not hold for small asphaltene particles ( $d < 3$  nm) because they tend to form non-uniform multilayers with possible viscoelastic characteristics.

## 1. Introduction

The adsorption kinetics of petroleum fluids is influenced by a number of factors, such as fluid composition and surface type.<sup>1</sup> In the absence of water, asphaltene–solid interactions can be described by two mechanisms: (1) polar interactions and (2) colloidal interactions near the onset of asphaltene flocculation.<sup>2</sup> The contribution of each mechanism depends upon the solvent quality of the oil with respect to asphaltene stability. In toluene, where asphaltenes are stable, polar interactions are likely to dominate the adsorption of asphaltenes onto solid surfaces. At relatively low concentrations, the adsorption kinetics of petroleum fluids in toluene usually stabilizes to a plateau value and generates Langmuir-type isotherms. The thickness of the adsorbed films is small ( $\sim 3$ – $5$  nm for medium crudes) and can be determined with a quartz crystal microbalance (QCM) after performing liquid-loading corrections.<sup>1</sup> However, the method is usually time-consuming, and the lifetime of QCM crystals is very limited because of irreversible adsorption of asphaltenes on their surface.

The objective of this work is to relate the thickness of adsorbed asphaltenes on QCM gold crystals to physical characteristics of asphaltenes in the bulk phase that are usually easier to determine. In a previous work, the adsorption of petroleum fluids on gold was found to be diffusion-controlled up to about 1000 ppm asphaltenes in toluene.<sup>1</sup> Diffusion-controlled adsorption is a process by which adsorbing species diffuse and adsorb onto a surface. Thus, it indicates a high affinity of particles to an interface. This usually occurs when the kinetic process inside the bulk solution is slower than at the interface. In this case, the Stokes translational diffusion coefficient of adsorbing species can

be estimated from early time adsorption kinetics.<sup>3</sup> On the other hand, the Stokes translational diffusion coefficient of electrically charged species in the bulk fluid can be determined from the speed of migration of these species under the action of an external electric field using the Nernst–Einstein equation.<sup>4</sup> If polar interactions are indeed key players in the adsorption process, then one can relate the dynamic adsorption of petroleum fluids to the direct-current (DC) conductivity of their ionic species. The DC conductivity can be measured with a high-precision impedance spectroscopic (IS) technique.<sup>4,5</sup> The main advantages of this method lay in the fact that it is fast and requires very small amounts of sample (4 mL). The average diameter of adsorbed particles can be estimated from the DC conductivity and diffusion coefficient using the Stokes–Einstein equation, provided that the ionic fraction of asphaltenes is known. For monolayer adsorption of spherical particles, the average diameter of adsorbed particles is comparable to their thickness.

This paper is structured into two main parts. In the first part, the ionic fraction of asphaltenes in toluene is estimated by comparing the size calculated from DC conductivity to the average size determined from direct imaging with atomic force microscopy (AFM). In the second part, the thicknesses of adsorbed films from 0.1 wt % asphaltenes in toluene from various crudes are measured by QCM and related to their DC conductivities determined by impedance spectroscopy.

## 2. Experimental Section

**2.1. Materials.** Materials include toluene, methylene chloride, *n*-heptane, all 99.9% HPLC grade from Fisher Scientific, acetone

\*To whom correspondence should be addressed. Telephone: 307-766-3278. E-mail: lgoual@uwyo.edu.

(1) Abudu, A.; Goual, L. Adsorption of crude oil on surfaces using quartz crystal microbalance with dissipation (QCM-D) under flow conditions. *Energy Fuels* **2009**, 23 (3), 1237.

(2) Buckley, J. S. Wetting alteration of solid surfaces by crude oils and their asphaltenes. *Rev. Inst. Fr. Pet.* **1998**, 53 (3), 303.

(3) Ward, A. F. H.; Tordai, L. Time dependence of boundary tensions of solutions. I. The role of diffusion in time effects. *J. Chem. Phys.* **1946**, 14 (7), 453.

(4) Goual, L. Impedance spectroscopy of petroleum fluids at low frequency. *Energy Fuels* **2009**, 23 (4), 2090.

(5) Zeng, H.; Song, Y. Q.; Johnson, D. L.; Mullins, O. C. Critical nanoaggregate concentration of asphaltenes by direct-current (DC) electrical conductivity. *Energy Fuels* **2009**, 23 (3), 1201.

Table 1. Properties of Selected Crude Oils

property	Chevron C	Mex-2	Tensleep	WP	WTx
density at 23 °C (g/cm <sup>3</sup> )	0.8655	0.8698	0.8692	0.9214	0.8863
gravity (°API)	32.0	31.2	31.3	22.1	28.2
refractive index at 23 °C	1.4829	1.4842	1.4909	1.5222	1.5163
molecular weight (g/mol)					
crude	253	242	280	282	
<i>n</i> C <sub>7</sub> maltenes	350	345	370	379	
<i>n</i> C <sub>7</sub> asphaltenes	820	935	998	993	
viscosity at 23 °C (cP)	28	25	19	112	
acid number (mg of KOH/g of oil)	0.2	0.2	0.2	0.2	0.1
base number (mg of KOH/g of oil)	0.7	1.2	0.9	2.3	1.1
resins (wt %)	25.6	20.8	20.7	25.0	13.5
<i>n</i> C <sub>7</sub> asphaltenes (wt %)	2.4	3.4	3.2	7.9	11.1
resin/asphaltene ratio (R/A)	10.7	6.2	6.5	3.2	1.2

99.4% ultra resi-analyzed (J.T. Baker), and attapulugus clay 30/60 (Forcoven products). Five medium crude oils are selected: Chevron C from Colorado, Mex-2 from Mexico, Tensleep from Wyoming, WP from Alaska, and WTx from west Texas. The crudes are filtered with a 20–25  $\mu\text{m}$  pore-size Whatman filter paper (Fisher Scientific) prior to each measurement. The physical properties of these crudes are provided in Table 1. Densities, viscosities, and refractive indices are determined using a DMA 45 density meter (Anton-Paar, Ashland, VA), Cannon–Fenske viscometer (Fisher Scientific), and GPR12-70E high-temperature refractometer (Index Instruments Ltd., Cambridgeshire, U.K.), respectively. The molecular weight is measured with a 5009 Cryette wide range cryoscope (Precision Systems, Livermore, CA). The total acid and base numbers are measured with a Metrohm 808 Titrandot autotitrator (CH-9101 Herisau, Switzerland).

**2.2. Asphaltene and Resin Separation Procedure.** Asphaltenes are extracted from crude oils by mixing a known amount of crude oil with *n*-heptane at a volume ratio of 1:40. The mixture is allowed to equilibrate after stirring and left overnight at room temperature. It is then filtered under vacuum using a 0.2  $\mu\text{m}$  pore size Whatman filter paper. The filter cake is repeatedly washed with *n*-heptane until the effluent from the filter becomes colorless. The asphaltenes are recovered from the filter cake by dissolution in toluene and then dried after toluene evaporation. Resins are extracted from deasphalted crude oils by adsorption chromatography on attapulugus clay according to a modified American Society for Testing and Materials (ASTM) D-2007 procedure.<sup>6</sup>

**2.3. QCM.** The E4 model (Q-sense AB, Sweden) is used to measure the adsorption of crude oils and asphaltenes on AT-cut gold-coated QCM crystals. The instrument monitors in real time the resonant frequency and dissipation shifts at the third harmonic overtone. The calculated mass densities,  $\Gamma$ , and thicknesses,  $h$ , are corrected for liquid-loading effects according to a procedure presented elsewhere.<sup>1</sup>

**2.4. IS.** An Agilent 4294A high-precision impedance analyzer (from 40 Hz to 110 MHz) connected to a HP 16452A liquid fixture (from 20 Hz to 30 MHz) through a four-terminal BNC cable is used to measure the complex impedance of the system. The DC conductivity,  $\sigma_{\text{DC}}$ , is calculated from the cross-sectional area of electrodes ( $A = 0.001\,134\,\text{m}^2$ ), the gap between electrode ( $t = 10^{-3}\,\text{m}$ ), and the parallel resistance of the system,  $R_p$ , according to

$$\sigma_{\text{DC}} = \frac{t}{AR_p} \quad (1)$$

The parallel resistance is determined by fitting the impedance data to an equivalent circuit using Z-view software.<sup>4</sup> Assuming particles with a spherical shape, their effective diameter,  $d$ , is determined from the Nernst–Einstein and Stokes–Einstein

equations

$$d = \frac{xCN_A e^2}{3\pi\eta_s M\sigma_{\text{DC}}} \quad (2)$$

where  $N_A$  is Avogadro's number ( $6.022\,141\,8 \times 10^{23}$ ),  $e$  is the ionic charge ( $1.602\,176\,5 \times 10^{-19}\,\text{C}$ ),  $C$  is the concentration of particles,  $\eta_s$  is the viscosity of toluene,  $x$  is the ionic fraction of particles, and  $M$  is the molecular weight of asphaltene particles ( $\approx 0.9\,\text{kg/mol}$  from Table 1).

Assuming homogeneous monolayer coverage with spherical particles, the thickness,  $h$ , of the adsorbed layer is comparable to the diameter of the particles and, thus, can be estimated from eq 2, provided that the ionic fraction is known.

**2.5. AFM.** The surface morphology of adsorbed films on QCM crystals is studied using a Nanoscope multimode atomic force microscope (Digital Instruments, Culver City, CA). Images are captured in air at room temperature under tapping mode. The images are scanned at  $5 \times 5\,\mu\text{m}$  and then  $1 \times 1\,\mu\text{m}$  to obtain a better image resolution. The scan rate is 0.9 Hz using a silicon cantilever tip with a length of 200  $\mu\text{m}$  and v-shaped in configuration with a spring constant of  $\sim 42\,\text{N/m}$  and a resonant frequency of  $\sim 300\,\text{kHz}$ . Both amplitude and height signal images are captured, and the diameters are measured from different images captured at several locations on the crystal using NanoScope IIIa software version 4.22r2.<sup>7</sup> The size detection limit of the AFM instrument is about 0.1 nm.

**Substrate Preparation.** The substrates are fixed by a piece of double-sided adhesive tape on a mica sample magnetically attached to the AFM stage. The diameter and height distribution of the adsorbing species are analyzed using the section and the depth command of the NanoScope software. The section feature produces a cross-sectional view of the image along any desired line to learn about their surface profiles (see Figure 1). This is performed for several images placed at different positions, and an average size is obtained.

### 3. Results and Discussion

**3.1. Determination of the Ionic Fraction of Asphaltenes in Toluene.** The determination of the size of asphaltenes from their DC conductivity according to eq 2 requires the knowledge of the ionic fraction of asphaltenes in toluene,  $x$ . In this study, we propose to estimate the ionic fraction by fitting the size data calculated from DC conductivity to average sizes obtained by direct imaging of adsorbed asphaltenes on gold. For this aim, a QCM crystal with adsorbed particles from 43 mg/L asphaltenes in toluene is imaged by AFM. The gold surface morphology exhibiting the asphaltene film is shown in Figure 2. Two to three scans of sizes are imaged at different positions to have a better representation of the

(6) Goual, L.; Firoozabadi, A. Measurement of asphaltenes and resins, and dipole moment in petroleum fluids. *AIChE J.* **2002**, 2646.

(7) Nanoscope Command Reference Manual, version 4.2. Digital Instruments, Culver City, CA, 1996.

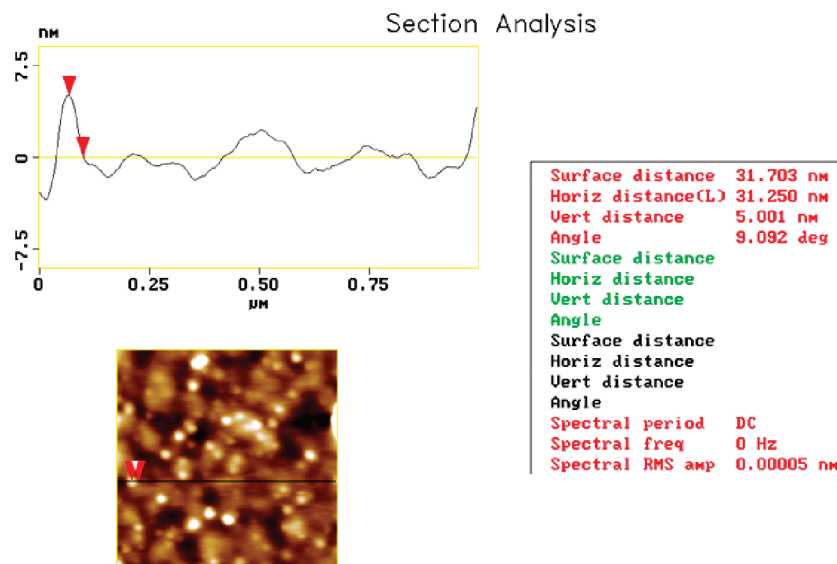


Figure 1. Determination of the size distribution of particles adsorbed on QCM gold crystals by AFM.

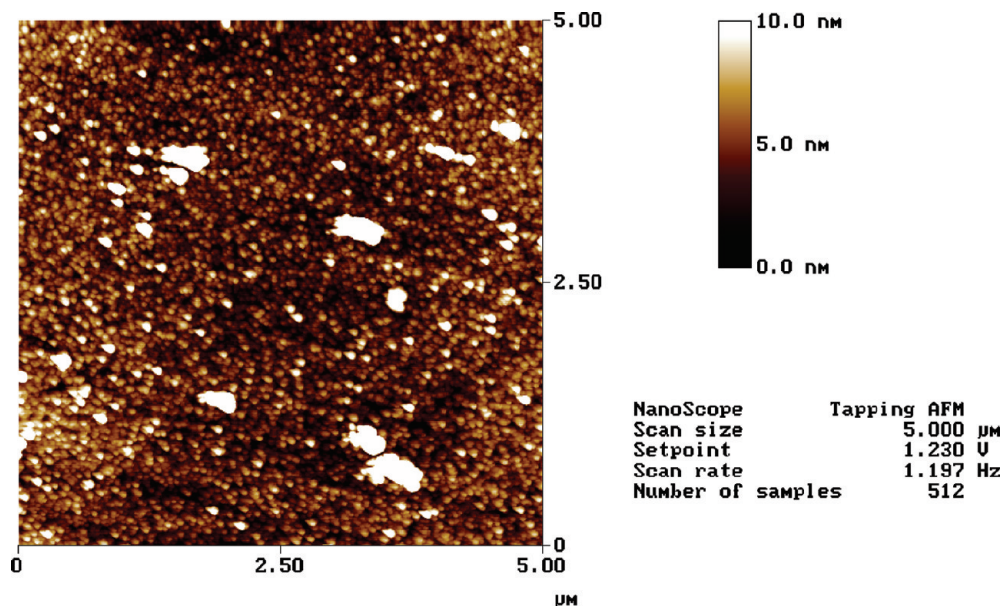


Figure 2. AFM image of adsorbed particles on gold from 43 mg/L asphaltenes in toluene.

surface morphology and distribution of particles. Asphaltene particles appear in the images as brown and white spherical particles. The sizes measured one by one are in the range of 2–40 nm and indicate a polydisperse system. However, the large sizes may be attributed to interparticle aggregation at the film surface.<sup>8</sup> The increase in particle size could also originate from the extra deposition left behind after evaporation of the solvent, leading to the formation of larger aggregates as the concentration increases.<sup>9</sup> Despite the polydispersity in size seen in Figure 2, we find that the proportion of large aggregates is relatively small. Instead, there is a large population of asphaltenes molecules and nanoaggregates with sizes between 2 and 6 nm. The average diameter is  $5 \pm 2$  nm, which is in reasonable agreement with data obtained from high-

Q ultrasonic, nuclear magnetic resonance (NMR) diffusion, and centrifugation.<sup>10–14</sup> Thus, from the conductivity standpoint, asphaltene particles can be represented by spherical particles of

(8) Batina, N.; Manzano-Martinez, J. C.; Andersen, S. I.; Lira-Galeana, C. AFM characterization of organic deposits on metal substrates from Mexican crude oils. *Energy Fuels* **2003**, *17*, 532.

(9) Kumar, K.; Dao, E.; Mohanty, K. K. AFM study of mineral wettability with reservoir oils. *J. Colloid Interface Sci.* **2005**, *289*, 206.

(10) Mullins, O. C.; Betancourt, S. S.; Cribbs, M. E.; Dubost, F. X.; Creek, J. L.; Andrews, B. A.; Venkataramanant, L. The colloidal structure of crude oil and the structures of oil reservoirs. *Energy Fuels* **2007**, *21* (5), 2785.

(11) Freed, D. E.; Lisitza, N. V.; Sen, P. N.; Song, Y.-Q. Molecular composition and dynamics of oils from diffusion measurements. In *Asphaltenes, Heavy Oils and Petroleomics*; Mullins, O. C., Sheu, E. Y., Hammami, A., Marshall, A. G., Eds.; Springer: New York, 2007.

(12) Lisitza, N. V.; Freed, D. E.; Sen, P. N.; Song, Y. Q. Self-assembly of asphaltenes: Enthalpy, entropy of depletion and dynamic at cross-over. *Magn. Reson. Imaging* **2007**, *25* (4), 544.

(13) Betancourt, S.; Ventura, G. T.; Pomerantz, A. E.; Vilorio, O.; Dubost, F. X.; Zou, J.; Monson, G.; Bustamante, D.; Purcell, J. M.; Nelson, R. K.; Rodgers, R. P.; Reddy, C. M.; Marshall, A. G.; Mullins, O. C. Nanoaggregates of asphaltenes in reservoir crude oil and reservoir connectivity. *Energy Fuels* **2009**, *23* (3), 1178.

(14) Mostowfi, F.; Indo, K.; Mullins, O. C.; McFarlane, R. Asphaltene nanoaggregates studied by centrifugation. *Energy Fuels* **2009**, *23* (3), 1194.



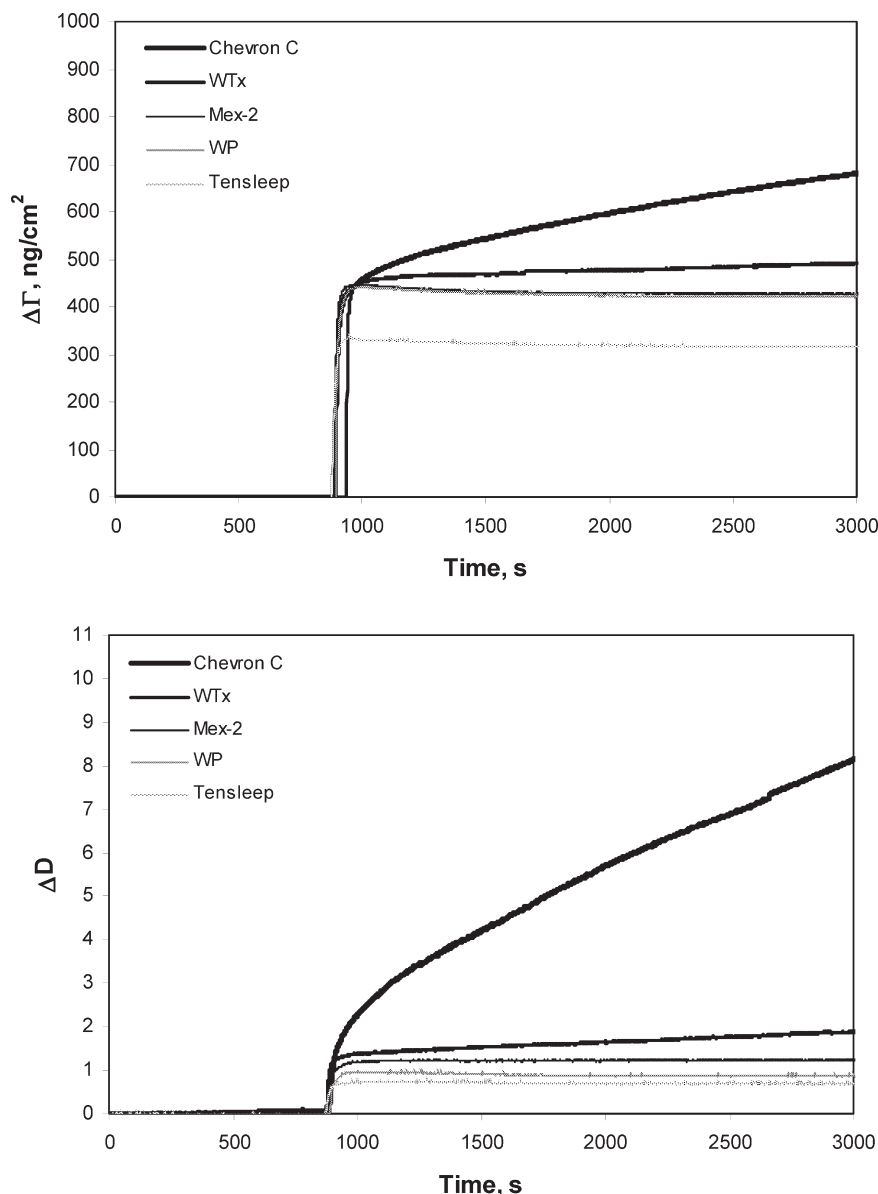


**Figure 3.** Adsorption kinetics of 0.1 wt % asphaltenes in toluene.

uniform size, density, and conductivity. From eq 2, the ionic fraction that would correspond to the average size measured is in the order of  $10^{-4}$ , which is higher than expected.<sup>5</sup> Note that this value would not change much if the molecular weight of asphaltenes was 750 g/mol instead of 900 g/mol. With this ionic fraction, the translational diffusion coefficient of asphaltene in toluene ( $\sim 10^{-10}$  m<sup>2</sup>/s) is comparable to those reported in the literature using other techniques.<sup>15–18</sup>

**3.2. Prediction of Adsorbed Film Thickness from DC Conductivity.** The adsorbed film thickness from 0.1 wt % asphaltenes in toluene is determined by QCM. The asphaltenes are extracted

from the crude oils presented in Table 1. Figure 3 depicts the adsorption kinetics of these asphaltenes in toluene. The data are obtained by simultaneous measurement of mass density variation ( $\Delta\Gamma$ ) and shift in dissipation ( $\Delta D$ ) with time at the third harmonic. Chevron C asphaltene exhibits a large mass density and dissipation shift that increase continuously with time. This may indicate multilayer adsorption and/or viscoelastic behavior. In contrast, the mass density of Mex-2, Tensleep, WP, and WTx asphaltenes stabilizes at a saturation plateau, and the relatively small dissipation shifts are mainly attributed to liquid-loading effects. The average thicknesses of these rigid films are corrected for liquid-loading effects and presented in Table 2 with 10% error. The film thicknesses obtained from different asphaltene nanoaggregates lie between 3 and 5 nm, in agreement with the literature.<sup>19,20</sup> Table 2 also contains the DC conductivity

(15) Groenzin, H.; Mullins, O. C. Asphaltenes molecular size and structure. *J. Phys. Chem. A* **1999**, *103*, 11237.

(16) Andrews, A. B.; Guerra, R. E.; Mullins, O. C.; Sen, P. N. Diffusivity of asphaltene molecules by fluorescence correlation spectroscopy. *J. Phys. Chem. A* **2006**, *110* (26), 8093.

(17) Badre, S.; Goncalves, C. C.; Norinaga, K.; Gustavson, G.; Mullins, O. C. Molecular size and weight of asphaltene and asphaltene solubility fractions from coals, crude oils and bitumen. *Fuel* **2006**, *85*, 1.

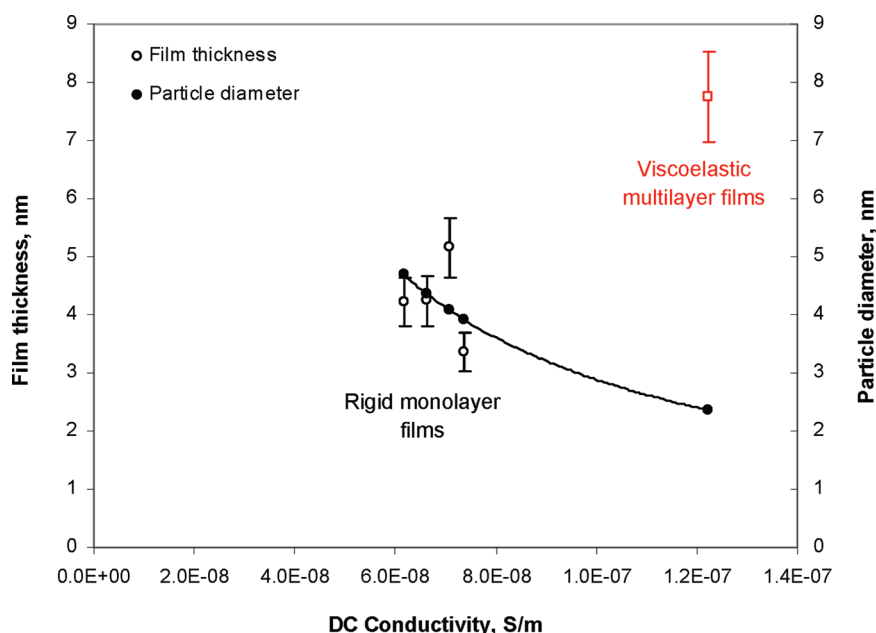
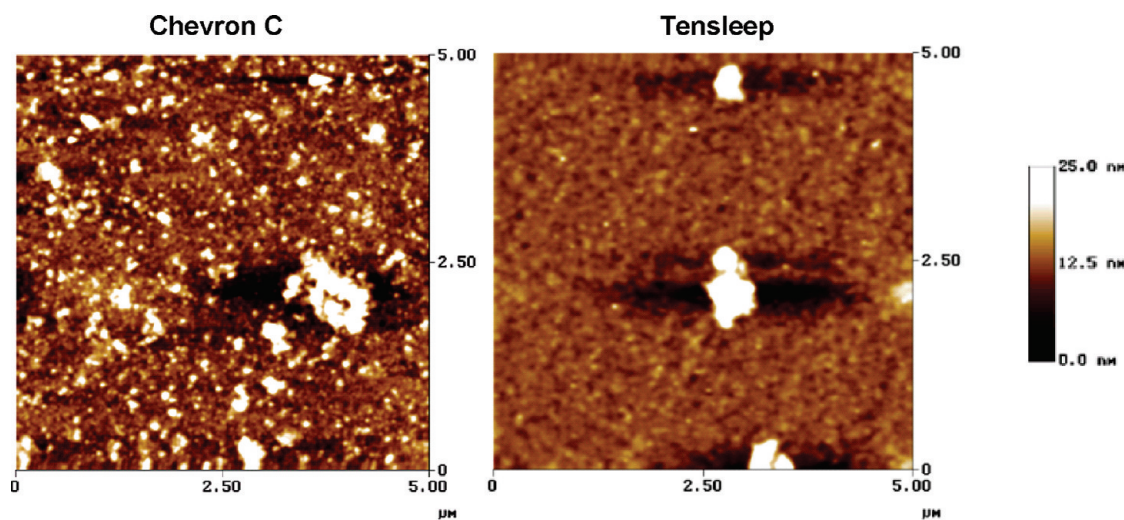
(18) Guerra, R. E.; Ladavac, K.; Andrews, A. B.; Mullins, O. C.; Sen, P. N. Diffusivity of coal petroleum asphaltene monomers by fluorescence correlation spectroscopy. *Fuel* **2007**, *86*, 2016.

(19) Hannisdal, A.; Ese, M.-H.; Hemmingsen, P. V.; Sjoblom, J. Particle-stabilized emulsions: Effect of heavy crude oil components pre-adsorbed onto stabilizing solids. *Colloids Surf., A* **2006**, *276*, 45.

(20) Simon, S.; Jestin, J.; Palermo, T.; Barre, L. Relation between solution and interfacial properties of asphaltene aggregates. *Energy Fuels* **2009**, *23* (1), 306.

**Table 2.** Adsorption Data and DC Conductivity of 0.1 wt % Asphaltenes in Toluene

	adsorption									conductivity	
	$\rho^{23}$ (g/cm <sup>3</sup> )	$\eta^{23}$ ( $\times 10^{-4}$ ) (mPa s)	$\Delta D$ ( $\times 10^{-6}$ )	$\Delta D_{\text{liqload}}$ ( $\times 10^{-6}$ )	$\Delta f$ (Hz)	$\Delta f_{\text{liqload}}$ (Hz)	$\Delta f_{\text{ads}}$ (Hz)	$\Delta \Gamma$ (ng/cm <sup>2</sup> )	$h$ (nm)	$\sigma_{\text{DC}}$ ( $\times 10^{-8}$ ) (S/m)	$d$ (nm)
Chevron C	0.86431	5.553	11.4	1.10	−139.82	−8	−131.58	776.29	7.76 at 9000 s	12.24	2.36
Mex-2	0.86427	5.602	1.22	1.61	−84.00	−12	−71.95	424.48	4.24	6.62	4.36
Tensleep	0.86431	5.569	0.74	1.27	−66.51	−10	−56.98	336.2	3.36	7.36	3.93
WP	0.86430	5.653	1.07	2.12	−87.53	−16	−71.60	422.44	4.22	6.16	4.69
WTx	0.86430	5.594	2.04	1.53	−98.82	−11	−87.38	515.53	5.16	7.07	4.08

**Figure 4.** Relation between film thickness, particle diameter, and DC conductivity of 0.1 wt % asphaltene in toluene.**Figure 5.** AFM images of adsorbed particles on gold from 0.5 wt % Chevron C and Tensleep crude oils in toluene.

of 0.1 wt % asphaltene in toluene determined from eq 1 and the diameter of asphaltene calculated from eq 2 using an ionic fraction of  $10^{-4}$ . We find that the thicknesses of adsorbed films are in the same range as the diameters of asphaltene, which indicates monolayer adsorption, in line with previous work.<sup>1,20</sup> Figure 4 shows the variations of thickness ( $h$ ) and diameter ( $d$ ) with DC conductivity. Assuming Langmuir-type adsorption of a monolayer of spherical particles with uniform size, the data can be fit to eq 2, which, for 0.1 wt % asphaltene in toluene,

simplifies to

$$h = \frac{3 \times 10^{-7}}{\sigma_{\text{DC}}} \quad (3)$$

On the other hand, the adsorbed film from Chevron C asphaltene does not follow this trend (see Figure 4). Indeed, the mass loading due to the adsorption of a rigid monolayer film is approximately 2.5 nm according to eq 3, which is

only 36% of the total adsorbed mass. To understand this behavior, AFM imaging of adsorbed films from 0.5 wt % Chevron C and Tensleep crudes in toluene is performed and illustrated in Figure 5. Tensleep crude is selected on the basis that its asphaltenes present the smallest mass and dissipation shifts on gold according to Figure 3. The images reveal a very different morphology of the two films. Tensleep film consists of a monolayer with few large aggregates scattered on its surface, whereas Chevron C film consists of a monolayer that is almost fully covered with a large number of small aggregates that possibly interact with each other. One may envisage non-uniform multilayer adsorption in this case. The very elevated dissipation shift recorded in Figure 3 may imply that the formed multilayer is soft (i.e., toluene-rich) and does not follow the oscillation of the sensor surface. This behavior is characteristic of viscoelastic films, whose mechanical properties are the subject of future research.

#### 4. Conclusions

A relation is established between the thickness of adsorbed rigid monolayer films on gold from different asphaltenes in

toluene and the DC conductivity of charged asphaltene species in the bulk fluid. When an ionic fraction of  $10^{-4}$  is considered, the thickness of adsorbed films is comparable to the diameters of asphaltenes calculated from DC conductivity. Thus, the method can be used as a quick tool to estimate the thickness of adsorbed rigid monolayer films on solids by simply measuring the DC conductivity of these fluids in the bulk phase. The relationship presented in this study is valid for the adsorption of 0.1 wt % asphaltenes on gold; however, the same procedure can be applied to other concentrations and surfaces. Because the IS method would underestimate the average size of asphaltenes in highly polydispersed systems, the concentrations should be maintained low enough (that is in the nanoaggregate range). Overall, the method is successful in predicting the adsorption of rigid asphaltene monolayers but fails to predict the adsorption of multilayers, which may occur when the particle diameters are smaller than 3 nm.

**Acknowledgment.** The authors would like to acknowledge the help of Patrick Johnson (University of Wyoming) for the use of QCM, and Carrick Eggleston (University of Wyoming) for the use of AFM.